Quantum calculation of the Vavilov-Cherenkov radiation by twisted electrons

I. P. Ivanov,[1] V. G. Serbo,[2,3] and V. A. Zaytsev[4,5]

[1]*CFTP, Instituto Superior Técnico, Universidade de Lisboa, Avenida Rovisco Pais 1, 1049-001 Lisbon, Portugal*

[2]*Novosibirsk State University, 630090 Novosibirsk, Russia*

[3]*Sobolev Institute of Mathematics, 630090 Novosibirsk, Russia*

[4]*Department of Physics, St. Petersburg State University, 7/9 Universitetskaya Nab., St. Petersburg 199034, Russia*

[5]*ITMO University, Kronverkskii Avenue 49, 197101 St. Petersburg, Russia*

(Received 24 February 2016; published 19 May 2016)

We present a detailed quantum electrodynamical description of Vavilov-Cherenkov radiation emitted by a relativistic twisted electron in the transparent medium. Simple expressions for the spectral and spectral-angular distributions as well as for the polarization properties of the emitted radiation are obtained. Unlike the plane-wave case, the twisted electron produces radiation within the annular angular region, with enhancement towards its boundaries. Additionally, the emitted photons can have linear polarization not only in the scattering plane but also in the orthogonal direction. We find that the Vavilov-Cherenkov radiation emitted by an electron in a superposition of two vortex states exhibits a strong azimuthal asymmetry. Thus, the Vavilov-Cherenkov radiation offers itself as a convenient diagnostic tool of such electrons and complements the traditional microscopic imaging.

DOI: 10.1103/PhysRevA.93.053825

I. INTRODUCTION

Soon after the discovery of Vavilov-Cherenkov (VC) radiation [1] it was explained by Frank and Tamm [2] within classical electrodynamics. A few years later, Ginzburg and Sokolov gave the quantum derivation of this phenomenon [3,4] and found quantum corrections to the classical Frank-Tamm result. The quantum electrodynamic description is presented in Ref. [5]. Since that time, many facets of Vavilov-Cherenkov radiation have been explored; see, for example, the old [6,7] and the more recent [8] reviews as well as monographs [9,10].

Although the quantum theory of Vavilov-Cherenkov radiation was worked out more than half a century ago, new theoretical publications on this topic still appear; see, for example, the very recent papers [11,12]. These works are in part driven by new experimental achievements that make it possible to observe and investigate the VC radiation under unusual circumstances. The VC radiation can then be accompanied by novel phenomena and other effects that were previously considered uninteresting are brought to the forefront. It is clear that these opportunities require the appropriate theoretical description.

In this work we develop the detailed quantum theory of the Vavilov-Cherenkov radiation emitted by vortex electrons. These are electron states whose wave function contains a topologically protected phase vortex and that carry orbital angular momentum (OAM) with respect to their average propagation direction. Following the suggestion of Ref. [13], vortex electron beams were experimentally demonstrated [14,15] and a number of remarkable effects that they produce were investigated [16]. Electromagnetic radiation of vortex electrons has not yet been investigated experimentally, but theoretical works suggest that it should display interesting effects in transition radiation [17,18] and Vavilov-Cherenkov radiation [11].

We undertook this study despite there being very recent work [11] on the same topic. In our paper, we perform a more complete study of the polarization properties, estimate the feasibility of observing the spectral cut-off and the discontinuity, and the spin-flip contributions mentioned in Ref. [11]. We also describe effects produced by radiating vortex electrons, namely, the diagnostic power of the VC radiation from vortex state superpositions, the spiraling pattern of the radiation of such electrons in the longitudinal magnetic fields, and the peculiar phenomenon of VC light concentration along the forward direction under an appropriate parameter choice.

In this paper we also present a more compact formalism than the one in the Supplemental Material of Ref. [11]. The formalism we use is based on the standard technology of helicity amplitude calculation and on the exact description of vortex electrons. We accurately set up the notation, pinpoint all nontrivial technical details that arise in the course of calculation, and provide physical insights for each interesting result.

The structure of the paper is as follows. In Sec. II we recall the standard quantum calculation of the VC radiation by plane-wave electrons and discuss the role of quantum corrections and the effect of non-plane-wave electrons. In Sec. III we repeat this analysis for the Bessel vortex electron and describe in detail the effects that arise there. Section IV contains a discussion of the results and a comparison with previous works. We summarize in Sec. V. Appendixes A and B contain detailed calculations for the fully polarized amplitude and for the case when all three particles are taken to be twisted.

II. VAVILOV-CHERENKOV RADIATION BY A PLANE-WAVE ELECTRON

A. Kinematics

The VC radiation can be treated within quantum electrodynamics (QED) as a decay process[1] $e(p) \to e(p') + \gamma(k)$

[1]It is interesting to note that this problem is very close to the computation of the equivalent photon density within the Weizsäcker-Williams approximation to QED processes [19,20].

(see, e.g., Ref. [9], Sec. 6). We use the following kinematical variables to describe the initial and final plane-wave states:

$$p=(E,\mathbf{p}),\quad p'=(E',\mathbf{p}'),\quad p^2=(p')^2=m_e^2,\quad v=|\mathbf{p}|/E, \tag{1}$$

$$k=(\omega,\mathbf{k}),\quad |\mathbf{k}|=\omega n,\quad k^2=-\omega^2(n^2-1)<0. \tag{2}$$

In this work we use the relativistic units $\hbar=1$ and $c=1$. The refraction index is frequency dependent $n=n(\omega)$, but we assume that the resulting dispersion is small $|\frac{\omega}{n}\frac{dn}{d\omega}|\ll 1$. We also assume that the medium is sufficiently transparent and homogeneous. The four-momentum conservation $p=p'+k$ is guaranteed by the in-medium modification of the photon dispersion relation. From this conservation law, we infer

$$k^2=-\omega^2(n^2-1)=2pk=2E\omega(1-vn\cos\theta_{kp}), \tag{3}$$

where θ_{kp} is the angle of the emitted photon with respect to the initial electron direction $\mathbf{pk}=|\mathbf{p}|\cdot|\mathbf{k}|\cos\theta_{kp}$. This angle is uniquely determined by the electron and photon energies $\theta_{kp}=\theta_0$, where

$$\cos\theta_0=\frac{1}{vn}+\frac{\omega}{2E}\frac{n^2-1}{vn}, \tag{4}$$

and is limited to $0<\theta_0<\pi/2$.

Now we recall how the QED calculation of this process proceeds. The initial plane-wave electron with helicity λ (the spin projection onto the electron momentum direction) is described by

$$\Psi_{\mathbf{p}\lambda}(x)=N_e u_{\mathbf{p}\lambda}e^{-ipx}, \tag{5}$$

where the bispinor $u_{\mathbf{p}\lambda}$ is normalized as $\bar{u}_{\mathbf{p}\lambda_1}u_{\mathbf{p}\lambda_2}=2m_e\delta_{\lambda_1,\lambda_2}$ and N is the normalization coefficient introduced below. The final electron is described by $\Psi_{\mathbf{p}'\lambda'}(x)$ and the emitted photon is described by the plane wave

$$A_\mu(x)=N_\gamma e_\mu e^{-ikx},\quad k^\mu e_\mu=0,\quad e^*_\mu e^\mu=-1. \tag{6}$$

The coefficients

$$N_e=\frac{1}{\sqrt{2E\mathcal{V}}},\quad N_{e'}=\frac{1}{\sqrt{2E'\mathcal{V}}},\quad N_\gamma=\frac{1}{n\sqrt{2\omega\mathcal{V}}} \tag{7}$$

correspond to the normalization of one particle per large volume $\mathcal{V}$. The scattering matrix element for this decay is [21]

$$\begin{aligned}S_{\rm PW}&=i\sqrt{4\pi\alpha}\int\overline{\Psi}_{\mathbf{p}'\lambda'}(x)\hat{A}^*(x)\Psi_{\mathbf{p}\lambda}(x)d^4x\\&=i(2\pi)^4\delta(p'+k-p)M_{fi}N_eN_{e'}N_\gamma,\\M_{fi}&=\sqrt{4\pi\alpha}\bar{u}_{\mathbf{p}'\lambda'}\hat{e}^*u_{\mathbf{p}\lambda},\end{aligned} \tag{8}$$

where a caret over a four-vector corresponds to its contraction with γ matrices, e.g., $\hat{A}=A_\mu\gamma^\mu$. Squaring the S-matrix element (8), dividing it by the total time, and integrating it over the final phase space gives the decay probability per unit time, that is, the decay width $\Gamma_{\rm PW}=dW_{\rm PW}/dt$. The normalization coefficients (7) together with the usual regularization prescription for the square of the four-momentum δ function guarantee that the final result does not depend on the normalization volume. Integration over the final electron three-momentum removes three of the four δ functions

$$\begin{aligned}&\int\delta(p'+k-p)d^3p'\\&=\delta(\tilde{E}'+\omega-E)=\frac{\tilde{E}'}{vE\omega n}\delta\left(\cos\theta_{kp}-\frac{1}{vn}-\frac{\omega}{2E}\frac{n^2-1}{vn}\right)\end{aligned} \tag{9}$$

and fixes the final electron energy $\tilde{E}'=\sqrt{\mathbf{p}^2+\mathbf{k}^2-2|\mathbf{p}||\mathbf{k}|\cos\theta_0+m_e^2}$. The spectral-angular distribution is then

$$\frac{d\Gamma_{\rm PW}}{d\omega d\Omega}=\frac{|M_{fi}|^2}{32\pi^2vE^2}\delta(\cos\theta_{kp}-\cos\theta_0). \tag{10}$$

This result corroborates the result (4) that, at given frequency ω, the photons are emitted, in the momentum space, along the surface of the cone with opening angle θ_0. This angle, of course, slightly depends on ω, due to both dispersion and the proximity to the cutoff frequency. Choosing the z axis along the initial electron direction and performing the integration over the photon polar angle θ_{kp}, we obtain

$$\frac{d\Gamma_{\rm PW}}{d\omega d\varphi_k}=\frac{|M_{fi}|^2}{32\pi^2vE^2}, \tag{11}$$

where φ_k is the azimuthal angle of the emitted photon.

B. Spectral-angular distribution

Evaluation of $|M_{fi}|^2$ represents a basic QED calculation and can be easily performed even when all particles are polarized. This fully polarized case is considered in Appendix A. Here we focus on the most relevant situation in which the initial electron is unpolarized and the final electron polarization is not detected. Then

$$\begin{aligned}|M_{fi}|^2&=4\pi\alpha\frac{1}{2}\sum_{\lambda\lambda'}|\bar{u}_{\mathbf{p}'\lambda'}\hat{e}^*u_{\mathbf{p}\lambda}|^2\\&=2\pi\alpha\,{\rm Tr}[(\hat{p}+m_e)\hat{e}(\hat{p}'+m_e)\hat{e}^*]\\&=4\pi\alpha(4|pe|^2+k^2e^*e).\end{aligned} \tag{12}$$

In the Coulomb gauge, the photon polarization vector is purely spatial $e^\mu=(0,\mathbf{e})$, with $\mathbf{e}^*\mathbf{e}=1$, and is orthogonal to the photon's direction $\mathbf{ke}=0$. Then the spectral-angular distribution takes the following form:

$$\frac{d\Gamma_{\rm PW}}{d\omega d\varphi_k}=\frac{\alpha}{2\pi}\left[\frac{|\mathbf{pe}|^2}{vE^2}+\frac{\omega^2}{4vE^2}(n^2-1)\right]. \tag{13}$$

This expression makes it clear that the emitted photon is linearly polarized in the scattering $(\mathbf{p},\mathbf{k})$ plane. Let us define the polarization vector $\mathbf{e}_\parallel$ lying in this plane and $\mathbf{e}_\perp$ orthogonal to it and the degree of linear polarization according to

$$P_l^{\rm PW}=\frac{d\Gamma^{(\parallel)}_{\rm PW}-d\Gamma^{(\perp)}_{\rm PW}}{d\Gamma^{(\parallel)}_{\rm PW}+d\Gamma^{(\perp)}_{\rm PW}}. \tag{14}$$

Then $P_l>0$ indicates that the light is (partially) polarized in the scattering plane, while $P_l<0$ corresponds to a partial polarization in the direction orthogonal to it. Evaluating the

above expression, we find

$$P_l^{\rm PW} = \frac{1}{1+d}, \quad d = \frac{1}{2}\left(\frac{\omega}{vE\sin\theta_0}\right)^2 (n^2-1). \tag{15}$$

Under the standard conditions, the first term in Eq. (13) dominates; the quantity d is then very small and the degree of linear polarization is close to 1.

It is not difficult to include the effects of the initial electron polarization (see Appendix A). It is known that, in the Weizsäcker-Williams approach, the equivalent photon acquires circular polarization proportional to the polarization of the initial electron [19,20]. One should expect the same effect for the Vavilov-Cherenkov radiation as well. The recent paper [12] claims that, in contradiction with this expectation, the emitted photons remain linearly polarized even with nonzero incoming electron polarization. This claim is incorrect and in Appendix A we analyze its origin.

Finally, if we do not detect the polarization of the final photon, we can sum the decay probability over its polarization states. The expression then becomes azimuthally symmetric and one arrives at the spectral distribution

$$\begin{aligned}\frac{d\Gamma_{\rm PW}}{d\omega} &= \alpha\left[v\sin^2\theta_0 + \frac{\omega^2}{2vE^2}(n^2-1)\right] \\ &= \frac{\alpha}{vn^2}\left[v^2n^2 - 1 - \frac{\omega}{E}(n^2-1) + \frac{\omega^2}{4E^2}(n^4-1)\right].\end{aligned} \tag{16}$$

C. Quantum corrections and the spectral cutoff

Comparing the spectral distribution (16) to the classical Frank-Tamm result $d\Gamma_{\rm cl}/d\omega = \alpha v[1-(vn)^{-2}]$, we see that

$$\frac{d\Gamma_{\rm PW}}{d\omega} = \frac{d\Gamma_{\rm cl}}{d\omega}(1-\eta), \quad \eta = \frac{\omega}{E}\frac{n^2-1}{v^2n^2-1} - \frac{\omega^2}{4E^2}\frac{n^4-1}{v^2n^2-1}, \tag{17}$$

thus η quantifies the relative magnitude of the quantum corrections. Under standard conditions, this factor is very small. Indeed, the sensitive medium used in the usual Cherenkov light detectors has refraction index $n \sim 1$ and they detect light that is emitted at a sizable polar angle, hence $vn - 1 \sim 1$, which for optical photons gives $\eta \lesssim 10^{-5}$. The relative magnitude of the quantum corrections can be increased by adjusting the expression $vn - 1$ to be very small, either for the usual media or with a simultaneous increase of the refraction index n. However, there are consequences for both options: The intensity of the VC radiation gets strongly suppressed. Just for illustration, we give estimates for three typical sets of parameters.

Example 1. This is the standard case. We detect radiation with $\omega = 2.25$ eV (green light) emitted with a moderately relativistic electron with $v = 0.9$ (kinetic energy of 661 keV) in a medium with refraction index $n = 1.46$. Then $vn - 1 = 0.31$, the spectral density $d\Gamma_{\rm PW}/d\omega = 0.38\alpha$, and the quantum correction $\eta = 3\times10^{-6}$, which can be safely neglected.

Example 2. This case borrows parameters from Ref. [11]. The wavelength is the same, the electron velocity is taken as $v = 0.685$, which corresponds to a kinetic energy of 190 keV, and the refraction index is highly tuned to be $n = 1.459\,86$. Under these conditions, the quantity $vn - 1$ drops by five order of magnitude $vn - 1 = 4.1\times10^{-6}$. The importance of quantum corrections increases up to $\eta = 0.44$, however the intensity $d\Gamma_{\rm PW}/d\omega = 3.1\times10^{-6}\alpha$, which is again five order of magnitude smaller than in the standard case. Also, the VC radiation is emitted at a small angle of $\theta_0 = 0.12^\circ$. Detection of the VC radiation under these special conditions brings up many serious technical challenges.

Example 3. Here we consider the same green light with $\omega = 2.25$ eV but emitted by a slow electron with $v = 0.0202$ (the kinetic energy is 104 eV) in a medium of very high refractive index $n = 50$. This value is not inconceivable as it can be achieved, for example, in metamaterials, but it remains unclear whether the medium is sufficiently transparent to make VC radiation detectable. In any event, for this choice we obtain $vn - 1 = 0.01$ and the quantum corrections are also large $\eta = 0.55$. The intensity in this case is less suppressed than in example 2 but is still small $d\Gamma_{\rm PW}/d\omega = 1.8\times10^{-4}\alpha$.

Another quantum effect is the presence of the spectral cutoff

$$\omega < \omega_{\rm cutoff} = 2E\frac{vn-1}{n^2-1}, \tag{18}$$

which simply follows from Eq. (4) by the requirement $\theta_0 > 0$. Its existence, of course, has been obvious for a long time and it is usually considered irrelevant because, under the standard conditions, $\omega_{\rm cutoff} \gtrsim 1$ MeV. In fact, for such energetic photons, even the starting assumption that the radiation can be treated as an electromagnetic response of a continuous medium with some refraction index is poorly justified.

However, it is conceivable that, by an appropriate medium choice, this cutoff frequency can be brought into the visible region, as in examples 2 and 3. In this case, the usual approach to the VC radiation is valid up to this cutoff. One then observes that the spectral density is discontinuous[2] at $\omega = \omega_{\rm cutoff}$. Indeed, just below the spectral cutoff, it takes the finite value

$$\frac{d\Gamma_{\rm PW}^{\rm cutoff}}{d\omega} = \alpha\frac{\omega_{\rm cutoff}^2}{2vE^2}(n^2-1) = \frac{2\alpha}{v}\frac{(vn-1)^2}{n^2-1}. \tag{19}$$

As $\omega \to \omega_{\rm cuoff}$, the emission angle $\theta_0 \to 0$ [see Eq. (4)] and both final particles move along the same axis z. The angular momentum conservation then immediately leads to

$$\lambda = \lambda' + \lambda_\gamma, \tag{20}$$

[2]The authors of [11] claim that this discontinuity is a novel feature arising due to the wave-packet nature of the vortex electron: "Immediately below this cutoff, we find a discontinuity in the radiation spectrum, presenting a clear deviation from the conventional ČR theory that displays no such cutoffs or discontinuities whatsoever." Here we demonstrate that, contrary to this claim, this discontinuity is not related to the wave-packet nature of the electron and does exist in the VC radiation emitted by the plane-wave electron. In general, the spectral distribution of the VC radiation emitted by any monochromatic electron wave packet must coincide with the plane-wave spectral distribution.

where λ, λ', and λ_γ are the helicities of the initial and final electron and of the emitted photon. This condition can only be satisfied by the helicity flip amplitudes, for which $\lambda_\gamma = 2\lambda = -2\lambda'$. Thus, the dominance of the spin-flip amplitude at the cutoff frequency comes from the helicity conservation in the strictly forward scattering and is part of the standard VC radiation treatment. This result also agrees with Eq. (15), which says that the degree of linear polarization $P_l^{\rm PW} \to 0$ as $\theta_0 \to 0$. The explicit expressions for these amplitudes are given in Appendix A.

Unfortunately, observation of the cutoff step of the spectral distribution faces huge experimental challenges, not only because one needs to bring $\omega_{\rm cutoff}$ down to the visible range but also because of the tiny intensity. For instance, within example 2, $\omega_{\rm cutoff} = 5.08$ eV, which is in the near-UV range, and from Eq. (19) we obtain $d\Gamma_{\rm PW}^{\rm cutoff}/d\omega = 4.3 \times 10^{-11}\alpha$, which agrees with the value read from Fig. 3(b) in Ref. [11]. In example 3, we get $\omega_{\rm cutoff} = 4.1$ eV and $d\Gamma_{\rm PW}^{\rm cutoff}/d\omega = 10^{-6}\alpha$, which is much larger but still strongly suppressed with respect to the standard case.

D. Role of wave packets

We close this section with a discussion of an aspect that, although being rather clear, is usually not discussed and therefore can cause some confusion, which we believe is illustrated by Ref. [11]. Both the classical treatment and the above quantum treatment of the Cherenkov radiation assume idealized nonphysical descriptions of the electron. The former approach treats the electron as a classical pointlike source of fields, while the latter assumes the electron to be a plane wave of infinite spatial extent. These two idealizations, despite being opposite to each other, lead to the same results, up to the tiny ω/E corrections.

This aspect is of course generic and not specific to VC radiation and it is not surprising that the results of the two approaches agree with each other. In any real experiment, an electron is a wave packet of certain transverse extent, which lies between the truly microscopic and macroscopic domains. It is true that the electron is not pointlike and it spreads as it propagates. However, under standard conditions, this spread is weak over experimental distances even if it moves in vacuum and is not subject to continuous interaction with the medium. Therefore, the electron usually does not spread to such an extent for which VC radiation would become very different from the pointlike source result.

In a similar fashion, the wave packet is not a true plane wave but is a superposition of such waves. The VC light emission from such an electron is an incoherent superposition of the radiation from individual plane-wave components (as we will see later for the vortex electron). Therefore, the wave-packet nature amounts only to some smearing of the angular distribution of the VC radiation.

In short, the fact that the electron is a wave packet provides *per se* a natural regularization to certain otherwise ill-defined quantities, but it does not lead to dramatic modification of the VC radiation properties. However, *structuring* this wave packet in a special way, one can strongly modify its angular distribution and this is where the vortex electrons lead to interesting results.

III. VAVILOV-CHERENKOV RADIATION BY A VORTEX ELECTRON

A. Kinematics

We now switch to the calculation of the VC radiation from the vortex electron case. We take the initial electron in the form of a cylindrical wave, known also as the Bessel vortex state (see details in Ref. [22]),

$$\Psi_{\varkappa m p_z \lambda}(x) = N_{\rm tw} \int \frac{d^2 p_\perp}{(2\pi)^2} a_{\varkappa m}(\mathbf{p}_\perp) u_{\mathbf{p}\lambda} e^{-ipx}, \qquad N_{\rm tw} = \sqrt{\frac{\pi}{2E\mathcal{R}\mathcal{L}_z}}, \tag{21}$$

where the Fourier amplitude is

$$a_{\varkappa m}(\mathbf{p}_\perp) = (-i)^m e^{im\varphi_p} \sqrt{\frac{2\pi}{\varkappa}} \delta(|\mathbf{p}_\perp| - \varkappa). \tag{22}$$

Note that the normalization coefficient $N_{\rm tw}$ differs from Eq. (7), but it still corresponds to one (Bessel-state) particle per large cylindrical volume $\mathcal{V} = \pi\mathcal{R}^2\mathcal{L}_z$. In this state, the electron moves, on average, along the axis z with the longitudinal momentum $p_z > 0$, while its transverse motion is represented by a superposition of plane waves with transverse momenta of equal modulus $\varkappa$ and various azimuthal angles φ_p. This state also possesses a definite energy $E = \sqrt{\varkappa^2 + p_z^2 + m_e^2}$, a definite helicity λ, and a definite value of the total angular momentum projection on the z axis: $J_z = m$, which is a half-integer.

The final electron and photon states are described, as before, by plane waves. This is the most appropriate choice for our physical problem, in which we integrate over the final electron states and ask for the photon's angular distribution.[3]

In this case, the S matrix is represented as a convolution of the plane-wave S matrix (8) with the Fourier amplitude $a_{\varkappa m}(\mathbf{p}_\perp)$:

$$S_{\rm tw} = i(2\pi)^4 \int \frac{d^2 p_\perp}{(2\pi)^2} \delta(p' + k - p) a_{\varkappa m}(\mathbf{p}_\perp) \times M_{fi}(p, p', k) N_{\rm tw} N_{e'} N_\gamma. \tag{23}$$

Squaring it and using the regularization procedure for the square of the δ function adapted to the Bessel states [23,24], we obtain

$$d\Gamma_{\rm tw} = d^3k \int_0^{2\pi} \frac{d\varphi_p}{2\pi} \frac{|M_{fi}(p, p', k)|^2}{32\pi^2 E \tilde{E}' \omega n^2} \delta(\tilde{E}' + \omega - E). \tag{24}$$

The expression (24) has one extra integration with respect to the plane-wave case, which modifies the angular distribution of the emitted radiation. This expression can be recast in the

[3]Formally, one can also represent the final photon by vortex states and predict its OAM distribution. However, experimental measurement of this distribution will hardly be possible with the modern technology as it requires a coherent macroscopic detector able to project the outgoing wave onto cylindrical states with different values of OAM.

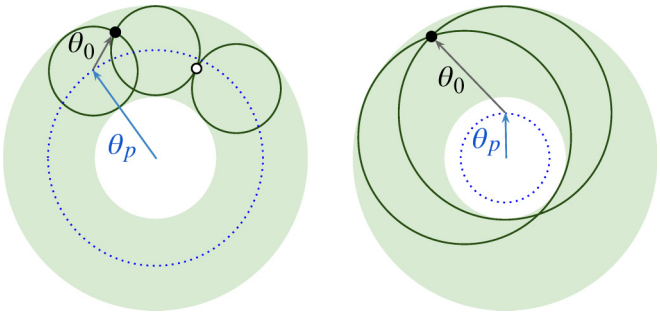

FIG. 1. Angular distribution of the VC radiation by a Bessel vortex electron with conical angle θ_p for $\theta_p > \theta_0$ (left) and $\theta_p < \theta_0$ (right). The dotted circle shows the opening angle of the vortex electron; the solid circles correspond to the VC cones from selected plane-wave configurations inside the vortex electron. Radiation going in every direction inside this region (black dot) receives contributions from two such plane-wave components. The white dot corresponds to the direction along which the polarization is orthogonal to the emission plane, $K = -1$ in Eq. (38).

very revealing form

$$\frac{d\Gamma_{\rm tw}}{d\omega d\Omega} = \int_0^{2\pi} \frac{d\varphi_p}{2\pi} \frac{d\Gamma_{\rm PW}}{d\omega d\Omega}. \tag{25}$$

This form makes it obvious that the spectral-angular distribution for the Bessel vortex state is given by an incoherent averaging over azimuthal angles of the plane-wave spectral-angular distributions for incoming electrons with fixed polar angle $\theta_p = \arctan(\varkappa/p_z)$.

Figures 1 and 2 help to visualize the angular distribution of the VC radiation from a Bessel vortex electron. In Fig. 1 we show this construction on the stereographic projection map, which is equivalent to the transverse plane for small polar angles, while in Fig. 2 we depict it in a three-dimensional side view. The two images of Fig. 1 correspond to the two cases depending on which of the opening angles, the plane-wave VC radiation angle θ_0 or the conical angle of the Bessel electron θ_p,

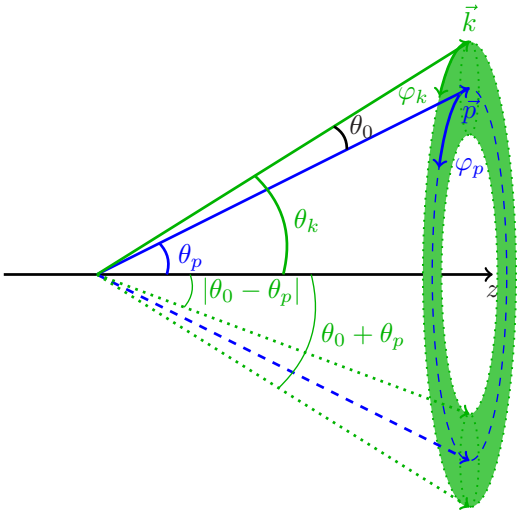

FIG. 2. Geometry of the VC emission by a vortex electron in a three-dimensional side view.

is the larger one. Every solid line circle corresponds to a single VC ring emitted by a particular plane-wave component; the envelope of all such circles represents the angular distribution for the Bessel electron.

Already this geometric construction makes it clear that in both cases $\theta_0 > \theta_p$ and $\theta_0 < \theta_p$ the radiation is emitted in the annual region with polar angles θ_k spanning from $|\theta_p - \theta_0|$ to $\theta_p + \theta_0$. In particular, for sufficiently large θ_0 and θ_p, one can have $\theta_p + \theta_0 > \pi/2$, which formally means that part of this radiation is emitted backward with respect to the average propagation direction of the initial vortex state. Certainly, this curious feature does not violate any known property of the VC radiation because, by construction, each such photon is emitted by an electron plane wave with large incidence angle.

B. Spectral-angular distribution

Let us now corroborate this geometric construction with analytical calculations. We substitute $d\Gamma_{\rm PW}$ in the form (10) into Eq. (25), express $\cos\theta_{kp}$ via the spherical angles of vectors $\mathbf{p}$ and $\mathbf{k}$, and perform the φ_p integration. We then encounter the integral

$$I = \int_0^{2\pi} f(\varphi_p)\delta(\cos\theta_0 - \sin\theta_k \sin\theta_p \cos(\varphi_p - \varphi_k) - \cos\theta_k \cos\theta_p)\frac{d\varphi_p}{2\pi}, \tag{26}$$

where $f(\varphi_p) = |M_{fi}|^2$, which, in general, depends on φ_p [see Eq. (12)]. There are only two φ_p points that contribute to this integral,

$$\varphi_p = \varphi_k \pm \delta, \quad \delta = \arccos\left(\frac{\cos\theta_0 - \cos\theta_k \cos\theta_p}{\sin\theta_k \sin\theta_p}\right). \tag{27}$$

Then the integral takes the simple form

$$I = \frac{f(\varphi_k + \delta) + f(\varphi_k - \delta)}{2} F(\theta_k,\theta_p,\theta_0), \tag{28}$$

where the function

$$F(\theta_k,\theta_p,\theta_0) = \frac{1}{\pi \sin\theta_k \sin\theta_p |\sin\delta|} \tag{29}$$

$$= \frac{1}{\pi} \{[\cos\theta_k - \cos(\theta_p + \theta_0)] \times [\cos(\theta_p - \theta_0) - \cos\theta_k]\}^{-1/2} \tag{30}$$

is symmetric under arbitrary permutations of its three arguments. It is nonzero only when they satisfy the triangle inequality

$$|\theta_p - \theta_0| < \theta_k < \theta_p + \theta_0. \tag{31}$$

It diverges at the borders of this interval, however this singularity is integrable, as

$$\int_{|\theta_p - \theta_0|}^{\theta_p + \theta_0} F(\theta_k,\theta_p,\theta_0) \sin\theta_k d\theta_k = 1. \tag{32}$$

This function has a minimum inside the annular region,

$$\min F(\theta_k,\theta_p,\theta_0) = \frac{1}{\pi \sin\theta_p \sin\theta_0} \quad \text{at} \quad \theta_k = \arccos(\cos\theta_p \cos\theta_0). \tag{33}$$

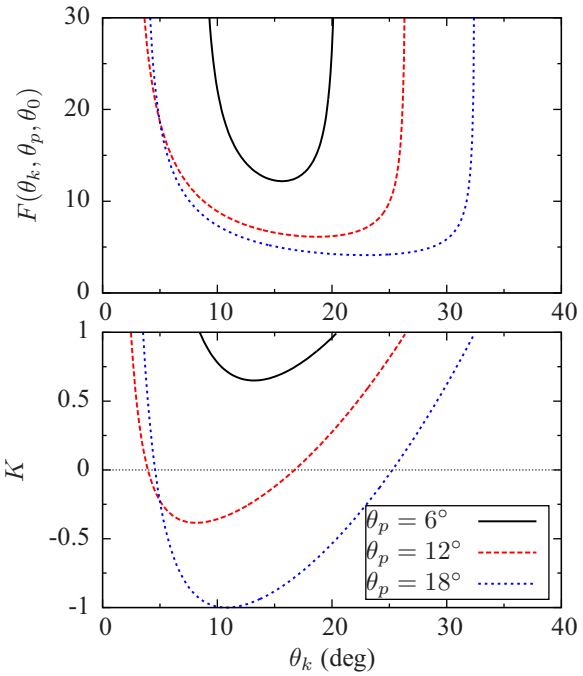

FIG. 3. Function $F(\theta_k,\theta_p,\theta_0)$ defined in Eq. (29) (top) and the quantity K defined in Eq. (37) (bottom) as functions of the photon polar angle for $\theta_0 = 14.5°$.

In Fig. 3 this function is plotted for various values of θ_p and for $\theta_0 = 14.5°$, which corresponds to $\omega = 2.25$ eV (green light), a refraction index of $n = 1.33$ (water), and a electron kinetic energy of 300 keV ($v = 0.78$), which is typical for electron microscopes. The spectral-angular distribution for the vortex electron VC radiation can then be compactly written as

$$\frac{d\Gamma_{\rm tw}}{d\omega d\Omega} = \frac{\alpha}{2\pi v}\left[\frac{\langle|\mathbf{pe}|^2\rangle}{E^2} + \frac{\omega^2}{4E^2}(n^2-1)\right]F(\theta_k,\theta_p,\theta_0), \quad (34)$$

where

$$\langle|\mathbf{pe}|^2\rangle = \tfrac{1}{2}\left(|\mathbf{pe}|^2|_{\varphi_p=\varphi_k+\delta} + |\mathbf{pe}|^2|_{\varphi_p=\varphi_k-\delta}\right). \quad (35)$$

C. Polarization properties

The expression (34) is convenient for the two choices of the photon linear polarization vector:[4] $\mathbf{e}_\parallel$ lying in the scattering plane spanned by the z axis and the vector $\mathbf{k}$, and $\mathbf{e}_\perp$ orthogonal to it. With these definitions, we can again calculate the degree of linear polarization

$$P_l^{\rm tw} = \frac{d\Gamma_{\rm tw}^{(\parallel)} - d\Gamma_{\rm tw}^{(\perp)}}{d\Gamma_{\rm tw}^{(\parallel)} + d\Gamma_{\rm tw}^{(\perp)}} = \frac{K}{1+d} = K\,P_l^{\rm PW}, \quad (36)$$

[4]Strictly speaking, the polarization state of a non-plane-wave photon is characterized by the polarization field rather than the polarization vector. With the full rigor, our definitions correspond to the so-called radial polarization for the former choice and the azimuthal polarization for the latter choice. However, when we discuss angular distribution, we have already selected a direction of the photon and defined a polarization vector at that point.

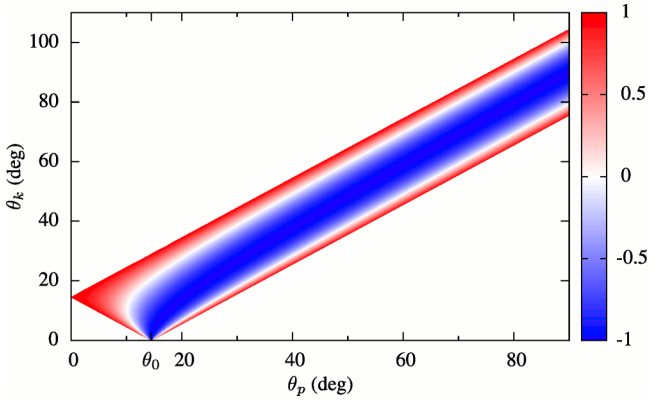

FIG. 4. Degree of linear polarization $P_l^{\rm tw}$ for a range of angles θ_k and θ_p for the same parameter choice as before.

where the quantity

$$K = 2\frac{(\cos\theta_k\cos\theta_0 - \cos\theta_p)^2}{\sin^2\theta_k\sin^2\theta_0} - 1 \quad (37)$$

describes how the degree of linear polarization for VC photons emitted in a given direction is modified when we switch from the plane wave to the vortex electron. This quantity is plotted in the bottom graph of Fig. 3. It always satisfies the condition $-1 \leqslant K \leqslant 1$. It attains its maximal value $K = 1$ at the borders of the interval (31), while its minimal value depends on the relation between θ_0 and θ_p:

$$\min K = -1 \quad \text{at } \cos\theta_k = \frac{\cos\theta_p}{\cos\theta_0} \quad \text{for } \theta_p > \theta_0, \quad (38)$$

$$\min K = 1 - 2\frac{\sin^2\theta_p}{\sin^2\theta_0} \quad \text{at } \cos\theta_k = \frac{\cos\theta_0}{\cos\theta_p} \quad \text{for } \theta_p < \theta_0. \quad (39)$$

Notice that negative values of K correspond to the linear polarization that is orthogonal to the scattering plane, a situation that is impossible for usual plane-wave scattering. This peculiar feature is however of purely kinematical origin and arises from the mismatch of the true scattering plane (that is, the plane formed by the direction of the photon and of the electron plane-wave component emitting this photon) and the overall scattering plane (the direction between the photon and the average direction of the vortex electron state). The point corresponding to the value $K = -1$ is also shown in Fig. 1 with a white dot. For completeness, we also show in Fig. 4 the degree of linear polarization as a function of the vortex electron opening angle and the polar angle of the emitted photon.

Alternatively, one can describe the emitted photon polarization in terms of definite helicity states $\lambda_\gamma = \pm 1$, which are described by vectors $\mathbf{e}^{(\pm)} = \mp(\mathbf{e}_\parallel \pm i\mathbf{e}_\perp)/\sqrt{2}$. One then checks that the spectral-angular distribution is independent of the helicity $d\Gamma_{\rm tw}^{(+)} = d\Gamma_{\rm tw}^{(-)}$ and is azimuthally symmetric. From here, just by multiplying by 2, one immediately obtains the spectral-angular distribution summed over the final photon

polarizations

$$\frac{d\Gamma_{\rm tw}}{d\omega d\Omega} = 2\frac{d\Gamma^{(\pm)}_{\rm tw}}{d\omega d\Omega} = \frac{\alpha}{2\pi}\left[v\sin^2\theta_0 + \frac{\omega^2}{2vE^2}(n^2-1)\right] \times F(\theta_k,\theta_p,\theta_0). \quad (40)$$

The spectral distribution can be obtained after an angular integral with the aid of Eq. (32). There exists however a more direct way. We notice that after summation over photon polarizations $d\Gamma_{\rm PW}$ does not depend on the $\mathbf{p}$ direction. Therefore, the φ_p integration of Eq. (25) is immediately performed and we obtain

$$\frac{d\Gamma_{\rm tw}}{d\omega} = \frac{d\Gamma_{\rm PW}}{d\omega} = \alpha\left[v\sin^2\theta_0 + \frac{\omega^2}{2vE^2}(n^2-1)\right]. \quad (41)$$

In short, the spectral distribution of the VC radiation by the twisted electron is identical to the plane-wave case.

D. Vavilov-Cherenkov radiation by a superposition of two vortex states

Let us consider now the case when the incoming electron is not a J_z eigenstate but is a superposition of two such states with different values m_1 and m_2 but with the same $\varkappa$ and p_z and therefore with the same energy $E=\sqrt{\varkappa^2+p_z^2+m_e^2}$. This state corresponds to a modification of Eq. (21) in which $a_{\varkappa m}(\mathbf{p}_\perp)$ is replaced by

$$c_1 a_{\varkappa m_1}(\mathbf{p}_\perp) + c_2 a_{\varkappa m_2}(\mathbf{p}_\perp), \quad c_i = |c_i|e^{i\alpha_i}, \quad |c_1|^2+|c_2|^2 = 1. \quad (42)$$

This leads to an additional factor under the φ_p integral in Eqs. (25) and (26):

$$G(\varphi_p) = 1 + 2|c_1c_2|\cos[\Delta m(\varphi_p - \pi/2) + \Delta\alpha], \quad (43)$$

where $\Delta m = m_2 - m_1$ and $\Delta\alpha = \alpha_2 - \alpha_1$.

For simplicity, we limit ourselves to the case when the photon polarization is not detected; if needed, the polarization dependence can be studied in the same manner as before. Then expression (28) contains an additional factor

$$2\pi\,\Phi(\varphi_k) = \tfrac{1}{2}[G(\varphi_k+\delta) + G(\varphi_k-\delta)] = 1 + A\cos[\Delta m(\varphi_k - \pi/2) + \Delta\alpha], \quad (44)$$

$$A = 2|c_1c_2|\cos(\delta\Delta m). \quad (45)$$

The spectral-angular distribution (40) then takes the following form:

$$\frac{d\Gamma_{\rm tw}}{d\omega d\Omega} = \alpha\left[v\sin^2\theta_0 + \frac{\omega^2}{2vE^2}(n^2-1)\right]F(\theta_k,\theta_p,\theta_0)\Phi(\varphi_k). \quad (46)$$

Thus, we observe the appearance of *azimuthal asymmetry* in the VC radiation of such electrons. This asymmetry depends on $\Delta m = m_2 - m_1$ as well as on the phase difference $\Delta\alpha = \alpha_2 - \alpha_1$ and its magnitude is quantified by A in Eq. (45), which, by definition, satisfies $|A| \leqslant 1$.

The spectral-angular distribution over the spherical angles of the emitted photons (θ_k,φ_k) is shown in Fig. 5 for $\theta_p = \theta_0/2$, $\Delta m = \pm 3$, $\Delta\alpha = \pi/2$, and $|c_1| = |c_2| = 1/\sqrt{2}$ and in Fig. 6 for $\Delta m = 3$, $\Delta\alpha = 0$, and $|c_1| = |c_2| = 1/\sqrt{2}$. Finally,

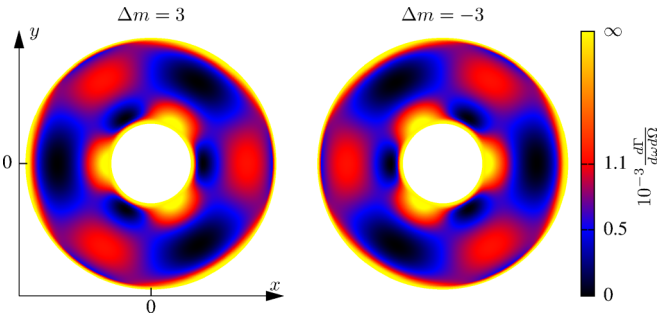

FIG. 5. Spectral-angular distribution as a function of emitted photon spherical angles θ_k and φ_k for $\theta_p = \theta_0/2$ and for the superposition with $\Delta m = \pm 3$, $\Delta\alpha = \pi/2$, and $|c_1| = |c_2| = 1/\sqrt{2}$.

as expected, the dependence on Δm and $\Delta\alpha$ disappears after the integration over the photon directions

$$\int F(\theta_k,\theta_p,\theta_0)\Phi(\varphi_k)d\Omega = 1 \quad (47)$$

and we are back to the spectral distribution (41).

IV. DISCUSSION

A. Vavilov-Cherenkov radiation as a diagnostic tool

The results of the previous section make the VC radiation a convenient macroscopic diagnostic tool for electron vortex beams. By measuring the parameters of the annular region, one can determine the angles θ_p and θ_0 and deduce from them the energy E and the conical momentum $\varkappa$ of the vortex electron.

This method is also very convenient for checking that the vortex electron is indeed in a superposition of several OAM states. Such superpositions can be cleanly prepared in modern electron microscopes and, when propagating in the longitudinal magnetic field, they display the OAM-induced Larmor and Gouy rotations [25]. They can also be used in subsequent scattering experiments on a solid target, where, as shown in [22], this superposition results in the azimuthal asymmetry of the scattering cross section.

The conventional method for detecting that a tightly focused electron beam is in an OAM-superposition state is to place a screen in the focal plane of the electron microscope and

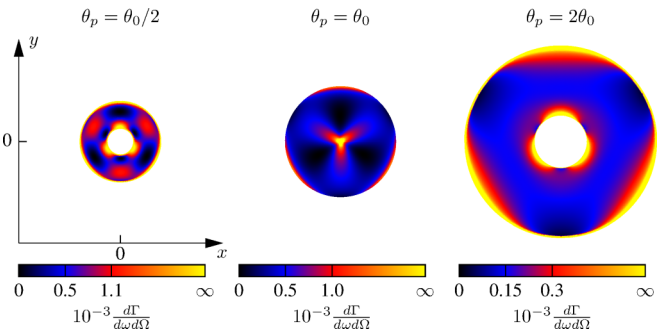

FIG. 6. Spectral-angular distribution as a function of emitted photon spherical angles θ_k and φ_k for the superposition with $\Delta m = 3$, $\Delta\alpha = 0$, and $|c_1| = |c_2| = 1/\sqrt{2}$. The size of the circle is proportional to θ_k.

detect the multipetal image. This is a microscopic observation method. Our calculations show that VC radiation from such electrons offers a complementary, macroscopic diagnostic tool that reveals the OAM-superposition state even for tightly focused electrons.

It is known that the VC radiation is emitted when the charged particle moves not only inside the medium, but also in its close vicinity, for example, through a microscopic channel inside a solid transparent medium [7,9,26,27]. Therefore, the method described above can be regarded as a nonintercepting one, since the electrons are allowed to pass through. As a result, it provides a convenient method to measure the OAM-induced Larmor and Gouy rotations of the vortex electrons [25]. The existing approach requires repeated measurements with fluorescent screens placed at different distances downstream the beam. Here the same effect can be detected in a single macroscopic experiment. As the multipetal electron beam propagates and rotates, the lobes of its VC radiation rotate correspondingly. The VC radiation emitted by the electron just entering the channel impinges on the outer regions of an end-cap photodetector, while the radiation emitted just before leaving the channel impinges on its innermost region. Since the lobes rotate as the electron propagates in the channel, a single large-area pixelized end-cap photodetector will show a *spiraling* VC radiation pattern.

The proposed type of experiment can also be used beyond vortex state superpositions to detect, in a macroscopic fashion, other forms of tightly focused coherently structured electron beams. The current state-of-the-art techniques of electron wave function manipulation inside electron microscopes allow one to prepare structured electron states with various predefined spatial or momentum distributions [16] and a complementary macroscopic detection technique will be welcome in this field.

B. Cherenkov concentrator

By appropriately adjusting the parameters, one can reach the regime of $\theta_p = \theta_0$. In this case, the annular region shown in Fig. 1 becomes the full disk and the VC radiation can be emitted arbitrarily close to the axis z of the average direction of the vortex electron. In the vicinity of this direction, that is, at small $\theta_k \ll 1$, the function $F(\theta_k,\theta_p = \theta_0,\theta_0)$ is

$$F(\theta_k,\theta_p = \theta_0,\theta_0) = \frac{1}{2\pi \sin(\theta_k/2)} \frac{1}{\sqrt{\sin^2\theta_0 - \sin^2(\theta_k/2)}} \approx \frac{1}{\pi \sin\theta_0} \frac{1}{\theta_k}. \tag{48}$$

One observes a remarkable regime of VC radiation being concentrated near the forward direction (see the middle plot in Fig. 6). If one selects a very small solid angle near the forward direction $\theta_k \leqslant \vartheta$, $\Delta\Omega = \pi\vartheta^2 \ll 1$, then a small but sizable part $O(\vartheta)$ of the total emitted VC light will be emitted in this very small solid angle. As a result, we obtain a bright source of VC radiation aligned with the direction of the vortex electron. The degree of linear polarization of this light will be close to -1, that is, the polarization vector will be aligned in the azimuthal direction. The experimental observation of this peculiar regime of the VC radiation is possible with today's technology.

C. Comparison with the semiclassical approach

It is also interesting to compare our results with the semiclassical approach to the calculation of VC radiation from a vortex electron presented in Ref. [18] as a pedagogical example en route to the more complicated transition radiation. In that work the vortex electron was modeled by a point charge equipped with a magnetic moment μ. This emergent magnetic moment was taken to be proportional to the total angular momentum m, as was derived in the original work on semiclassical dynamics of vortex electron wave packets [13]. With this simplistic model, Ref. [18] recovered the Tamm-Frank result for the spectral distribution of the VC radiation from such a source, which, in our notation, can be written as

$$\frac{d\Gamma_{\text{tw;semicl}}}{d\omega} = \frac{d\Gamma_{\text{cl}}}{d\omega}\left[1 + \left(m\frac{\omega n}{2Ev}\right)^2\right] \tag{49}$$

and which describes the sum of the VC radiation intensities from the electric and magnetic currents.

Comparing this semiclassical expression with our results, we can make two observations. First, the extra term in Eq. (49) is suppressed by ω^2/E^2. For small m, it is smaller than the first quantum correction [see Eq. (17)] and keeping it would go beyond the approximations used in the semiclassical evaluation. However, for very large m, of the order of thousands (electron vortex beams with orbital angular momentum up to 100 were already observed in Refs. [15,28]), this contribution can overcome the quantum correction and keeping it will become legitimate. The calculations of Ref. [18] assume this regime.

Second, expression (49) explicitly depends on the vortex electron angular momentum m, while our results for vortex electrons are m independent. Even though the pure Bessel state, which we use, and the compact vortex wave packet used in Ref. [18] are different, the appearance of the m dependence is worrisome. We believe that this discrepancy signals the breakdown, for the VC radiation problem, of the semiclassical model, which views a vortex electron as a pointlike object with unresolved structure.

V. CONCLUSION

In this work we gave a full quantum mechanical treatment of the VC radiation emitted by a vortex electron and compared it with the standard plane-wave case. We investigated the spectral, angular, and polarization properties and discussed the roles of quantum effects, of the coherence, and of the non-plane-wave nature of the vortex state. We also gave transparent physical explanations to various effects the calculations lead to.

Taking the electron as a superposition of two vortex states, we found two remarkable effects: the possibility of a multipetal spiraling structure of the VC radiation emitted by such an electron in a longitudinal magnetic field and a remarkable concentration of the VC light in the forward direction when the opening angles of the electron vortex state and the VC cone match. Both effects can be observed with the existing technology. We also discussed the possibility of utilizing the VC radiation as a diagnostic tool for the determination of the vortex electrons parameters and for testing the purity of the vortex state.

Our paper contains not only results and physics insights but also a detailed exposition of the formalism appropriate for

calculation of VC radiation from vortex electrons. We hope we have presented and discussed enough technical details to enable the reader to repeat our calculations and to apply this machinery to other processes.

Finally, we discussed several claims made recently in the literature on the spectral, angular, and polarization properties the VC radiation as well as on the role of coherence, quantum corrections, and deviations of the VC radiation of non-plane-wave electrons from the plane-wave case.

ACKNOWLEDGMENTS

We are grateful to G. Kotkin, V. Prinz, and V. Telnov for useful discussions. The work of I.P.I. was supported by the Portuguese Fundação para a Ciência e a Tecnologia (FCT) through the FCT Investigator Contract No. IF/00989/2014/CP1214/CT0004 through the IF2014 Programme, as well as under Contracts No. UID/FIS/00777/2013 and No. CERN/FIS-NUC/0010/2015, which are partially funded through POCTI (FEDER), COMPETE, QREN, and the EU. I.P.I. is also thankful to Helmholtz Institut Jena for hospitality during his stay as a Visiting Professor funded by the ExtreMe Matter Institute EMMI, GSI Helmholtzzentrum für Schwerionenforschung, Darmstadt. V.G.S. acknowledges support from RFBR via Grant No. 15-02-05868. The work of V.A.Z. was supported by RFBR (Grant No. 16-02-00334) and by SPbSU (Grants No. 11.38.269.2014 and No. 11.38.237.2015).

APPENDIX A: VAVILOV-CHERENKOV RADIATION AMPLITUDE IN A FULLY POLARIZED SETUP

Here, for completeness, we derive the amplitude M_{fi} [see Eq. (8)] for the case when all particles are polarized. The initial and final electron helicities are denoted by λ and λ', respectively, while the photons are also taken to be circularly polarized with helicity λ_γ. Note that we consider the general kinematics, without aligning the initial electron along a predefined axis z.

The initial electron bispinor has the following form (see the derivation in Ref. [22]):

$$u_{\mathbf{p}\lambda} = \sum_{\sigma=\pm 1/2} e^{-i\sigma\varphi_p} d^{1/2}_{\sigma\lambda}(\theta_p) U^{(\sigma)}(E,\lambda), \tag{A1}$$

where $d^J_{MM'}(\theta)$ is the Wigner matrix [29,30] and the basis bispinors $U^{(\sigma)}(E,\lambda)$ are expressed as

$$U^{(\sigma)}(E,\lambda) = \begin{pmatrix} \sqrt{E+m_e}\, w^{(\sigma)} \\ 2\lambda\sqrt{E-m_e}\, w^{(\sigma)} \end{pmatrix},$$
$$w^{(+1/2)} = \begin{pmatrix} 1 \\ 0 \end{pmatrix}, \tag{A2}$$
$$w^{(-1/2)} = \begin{pmatrix} 0 \\ 1 \end{pmatrix}.$$

They do not depend on the direction of $\mathbf{p}$ and are eigenstates of the spin projection operator s_z with eigenvalues $\sigma = \pm 1/2$. The final electron bispinor $u_{\mathbf{p}'\lambda'}$ is constructed in a similar way. The polarization state of the photon is described in the same formalism (see details in Ref. [31])

$$\mathbf{e}_{\mathbf{k}\lambda_\gamma} = \sum_{\sigma_\gamma=0,\pm 1} e^{-i\sigma_\gamma\varphi_k} d^{\,1}_{\sigma_\gamma\lambda_\gamma}(\theta_k)\boldsymbol{\chi}_{\sigma_\gamma}, \tag{A3}$$

where the basis vectors

$$\boldsymbol{\chi}_0 = \begin{pmatrix} 0 \\ 0 \\ 1 \end{pmatrix}, \quad \boldsymbol{\chi}_{\pm 1} = \frac{\mp 1}{\sqrt{2}} \begin{pmatrix} 1 \\ \pm i \\ 0 \end{pmatrix} \tag{A4}$$

represent the eigenstates of the photon spin z-projection operator with the eigenvalues $\sigma_\gamma = 0, \pm 1$.

The scattering amplitude (8) takes then the form

$$\begin{aligned} M_{fi} &= -\sqrt{4\pi\alpha}\,\bar{u}_{\mathbf{p}'\lambda'}\hat{\mathbf{e}}^*_{\mathbf{k}\lambda_\gamma} u_{\mathbf{p}\lambda} \\ &= -\sqrt{4\pi\alpha} \sum_{\sigma\sigma'\sigma_\gamma} e^{i(\sigma'\varphi_{p'}+\sigma_\gamma\varphi_k-\lambda\varphi_p)} d^{1/2}_{\sigma\lambda}(\theta_p) \\ &\quad \times d^{1/2}_{\sigma'\lambda'}(\theta_{p'}) d^{\,1}_{\sigma-\sigma',\lambda_\gamma}(\theta_k) W^{(\sigma\sigma'\sigma_\gamma)}, \end{aligned} \tag{A5}$$

where

$$\begin{aligned} W^{(\sigma\sigma'\sigma_\gamma)} &= \overline{U}^{(\sigma')}(E',\lambda')(\boldsymbol{\gamma}\boldsymbol{\chi}^*_{\sigma_\gamma})U^{(\sigma)}(E,\lambda) \\ &= [2\lambda\sqrt{(E-m_e)(E'+m_e)} \\ &\quad + 2\lambda'\sqrt{(E'-m_e)(E+m_e)}] \\ &\quad \times [2\sigma(\delta_{\sigma,\sigma'} - \sqrt{2}\delta_{\sigma,-\sigma'})]\delta_{\sigma_\gamma,\sigma-\sigma'}. \end{aligned} \tag{A6}$$

which shows that each individual nonzero term in Eq. (A5) complies with the spin z-projection conservation law

$$\sigma = \sigma' + \sigma_\gamma. \tag{A7}$$

The triple summation in Eq. (A5) becomes effectively just a double summation over σ and σ'.

We can now simplify this general kinematics by selecting the z axis along the direction of the initial electron $\theta_p = \varphi_p = 0$. Then $d^{1/2}_{\sigma\lambda}(\theta_p) = \delta_{\sigma\lambda}, \varphi_{p'} = \varphi_k + \pi$, and the scattering amplitude becomes

$$\begin{aligned} M_{fi} &= -\sqrt{4\pi\alpha}[\sqrt{(E-m_e)(E'+m_e)} \\ &\quad + (2\lambda)(2\lambda')\sqrt{(E'-m_e)(E+m_e)}]e^{i\lambda\varphi_k} \sum_{\sigma'=\pm 1/2} e^{i\pi\sigma'} \\ &\quad \times d^{1/2}_{\sigma'\lambda'}(\theta_{p'}) d^{1}_{\lambda-\sigma',\lambda_\gamma}(\theta_k)(\delta_{\lambda,\sigma'} - \sqrt{2}\delta_{\lambda,-\sigma'}), \end{aligned} \tag{A8}$$

with θ_k and $\theta_{p'}$ related by $\omega n \sin\theta_k = |\mathbf{p}'| \sin\theta_{p'}$.

Here we remark that for the *strictly forward scattering*, which corresponds to the $\omega = \omega_{\text{cutoff}}$ limit, $d^{1/2}_{\sigma'\lambda'}(\theta_{p'}) = \delta_{\sigma',\lambda'}$ and $d^{\,1}_{\lambda-\sigma',\lambda_\gamma}(\theta_k) = \delta_{\lambda-\sigma',\lambda_\gamma}$ and therefore only the helicity flip amplitude survives:

$$\begin{aligned} M^{\text{forward}}_{fi} &= \sqrt{8\pi\alpha}[\sqrt{(E-m_e)(E'+m_e)} \\ &\quad - \sqrt{(E'-m_e)(E+m_e)}]e^{i\lambda(\varphi_k-\pi)}\delta_{\lambda',-\lambda}\delta_{\lambda_\gamma,2\lambda}. \end{aligned} \tag{A9}$$

This result is a straightforward consequence of the helicity conservation law, which is always expected at the cutoff frequency, and has nothing to do with the choice of the electron wave function. Thus, the spectral distribution approaches the

finite value in this limit

$$\frac{d\Gamma_{\rm PW}^{\rm forward}}{d\omega}=\frac{\left|M_{fi}^{\rm forward}\right|^2}{16\pi vE^2}=\frac{\alpha}{2v}\left(\frac{\omega}{E}\right)^2\frac{[vE-n(E+m_e)]^2}{(E+m_e)(E'+m_e)} \tag{A10}$$

and its value is suppressed by the small parameter $(\omega/E)^2$.

The helicity amplitudes derived above give a convenient basis to calculate this process for arbitrarily polarized particles. Let us assume that the initial electron has arbitrary polarization described by the 4-vector

$$a^\mu=(a_0,\mathbf{a}),\quad a_0=\frac{\mathbf{p}\boldsymbol{\zeta}}{m_e},\quad \mathbf{a}=\boldsymbol{\zeta}+\frac{(\mathbf{p}\boldsymbol{\zeta})}{m_e(E+m_e)}\mathbf{p}, \tag{A11}$$

where $\boldsymbol{\zeta}$ is twice the average value of the electron spin in its rest frame. In this case, the result (12) must be supplemented with an extra term

$$\Delta|M_{fi}|^2=-8\pi\alpha i m_e\varepsilon^{\mu\nu\alpha\beta}e_\mu^* e_\nu k_\alpha a_\beta. \tag{A12}$$

Clearly, this expression is zero when $e_\mu^*=e_\mu$, which corresponds to the linear polarization of the photon. For circularly polarized photons with $(e_\mu^{(\lambda_\gamma)})^*=-e_\mu^{(-\lambda_\gamma)}$, we get

$$\Delta|M_{fi}|^2=8\pi\alpha\lambda_\gamma m_e\omega\left(a_0 n-\frac{\mathbf{ak}}{\omega n}\right), \tag{A13}$$

where $\lambda_\gamma=\pm1$. The recent work in [12] assumes, without any justification, that $e_\mu^*=e_\mu$, which leads to the erroneous conclusion that the VC radiation does not acquire circular polarization even if the initial electron is polarized.

In fact, it does. To see this, we present the electron polarization vector as

$$\boldsymbol{\zeta}=\boldsymbol{\zeta}_\parallel+\boldsymbol{\zeta}_\perp,\quad \boldsymbol{\zeta}_\parallel=\mathbf{p}\frac{(\boldsymbol{\zeta}\mathbf{p})}{\mathbf{p}^2}=2\langle\lambda\rangle\frac{\mathbf{p}}{|\mathbf{p}|}, \tag{A14}$$

where $\langle\lambda\rangle$ is the average helicity of the initial electron. Then

$$\Delta|M_{fi}|^2=8\pi\alpha\lambda_\gamma\omega E\left[2\langle\lambda\rangle(vn-\cos\theta_0)-\frac{m_e}{E}\frac{\boldsymbol{\zeta}_\perp\mathbf{k}}{n\omega}\right]. \tag{A15}$$

The degree of the circular polarization of the VC photon is then

$$\begin{aligned}P_c^{\rm PW}&=\frac{d\Gamma_{\rm PW}^{(\lambda_\gamma=+1)}-d\Gamma_{\rm PW}^{(\lambda_\gamma=-1)}}{d\Gamma_{\rm PW}^{(\lambda_\gamma=+1)}+d\Gamma_{\rm PW}^{(\lambda_\gamma=-1)}}\\&=\frac{\omega}{Ev^2\sin^2\theta_0}\frac{2\langle\lambda\rangle(vn-\cos\theta_0)-\frac{m_e}{E}\frac{\boldsymbol{\zeta}_\perp\mathbf{k}}{n\omega}}{1+d}\end{aligned} \tag{A16}$$

and it is nonzero when the initial electron has a nonzero polarization $\boldsymbol{\zeta}\neq0$. Under normal conditions, this polarization is small. However, at the spectral cutoff and with $\langle\lambda\rangle=+1/2$, we get $P_c^{\rm PW}=+1$, in accord with Eq. (A9).

APPENDIX B: VAVILOV-CHERENKOV RADIATION AMPLITUDE IN THE ALL-VORTEX BASIS

All the above derivations were done for the VC radiation from plane-wave electrons and for arbitrary polarization of all particles. Here we present the construction of the S-matrix element for the arbitrarily polarized *vortex* states, including also the case when all three particles are twisted. Although this approach is not the most convenient one for calculation of the spectral-angular distribution, we give the results for the sake of completeness. We stress that they can be obtained by a direct combination of the formalisms and compilation of the results that are already known and published in Refs. [22,24,31].

Once again, the initial vortex electron is described by the Bessel state (21). In the cylindrical coordinates ρ,φ,z, it takes the following form (see details in Ref. [22]):

$$\begin{aligned}\Psi_{\varkappa mp_z\lambda}(\rho,\varphi,z,t)&=N_{\rm tw}e^{-iEt+ip_z z}\sqrt{\frac{\varkappa}{2\pi}}\sum_{\sigma=\pm1/2}(-i)^\sigma e^{i(m-\sigma)\varphi}\\&\times d^{1/2}_{\sigma\lambda}(\theta_p)J_{m-\sigma}(\varkappa\rho)U^{(\sigma)}(E,\lambda),\end{aligned} \tag{B1}$$

with the bispinor $U^{(\sigma)}(E,\lambda)$ defined in Eq. (A2). The similar function $\Psi_{\varkappa' m' p'_z\lambda'}(\rho,\varphi,z,t)$ describes the final electron. The Bessel vortex photon moving along the z axis with momentum k_z and having a definite modulus of the transverse momentum $\varkappa_\gamma$, definite energy $\omega=\sqrt{\varkappa_\gamma^2+k_z^2}$, and definite helicity λ_γ and the z projection of the total spin $J_z=m_\gamma$ is described by $A^\mu(x)=[0,\mathbf{A}(x)]$ (see details in Ref. [31]):

$$\begin{aligned}\mathbf{A}_{\varkappa_\gamma m_\gamma k_z\lambda_\gamma}(\rho,\varphi,z,t)&=N_{\rm tw}^\gamma\int\frac{d^2k_\perp}{(2\pi)^2}a_{\varkappa_\gamma m_\gamma}(\mathbf{k}_\perp)e^\mu_{\mathbf{k}\lambda_\gamma}e^{-ikx}\\&=N_{\rm tw}^\gamma e^{-i\omega t+ik_z z}\sqrt{\frac{\varkappa_\gamma}{2\pi}}\sum_{\sigma_\gamma=0,\pm1}(-i)^{\sigma_\gamma}\\&\times e^{i(m_\gamma-\sigma_\gamma)\varphi}d^1_{\sigma_\gamma\lambda_\gamma}(\theta_k)J_{m_\gamma-\sigma_\gamma}(\varkappa_\gamma\rho)\boldsymbol{\chi}_{\sigma_\gamma},\end{aligned} \tag{B2}$$

where the normalization coefficient is

$$N_{\rm tw}^\gamma=\frac{1}{n}\sqrt{\frac{\pi}{2\omega\mathcal{R}\mathcal{L}_z}} \tag{B3}$$

and the vectors $\boldsymbol{\chi}_{\sigma_\gamma}$ are defined in Eq. (A4).

The S-matrix element for the fully twisted process is obtained by substituting these expressions into the integral

$$\begin{aligned}S_{3\rm tw}&=i\sqrt{4\pi\alpha}\int\overline{\Psi}_{\varkappa' m' p'_z\lambda'}(\rho,\varphi,z,t)\hat{A}^*_{\varkappa_\gamma m_\gamma k_z\lambda_\gamma}(\rho,\varphi,z,t)\\&\times\Psi_{\varkappa mp_z\lambda}(\rho,\varphi,z,t)\rho\,d\rho\,d\varphi\,dz\,dt.\end{aligned} \tag{B4}$$

As usual, the t and z integrals immediately lead to the energy and longitudinal momentum conservation laws $E'+\omega=E$ and $p'_z+k_z=p_z$, respectively. Integration over φ leads to the conservation of the z projection of the total angular momentum in each individual term of this sum:

$$m'-\sigma'+m_\gamma-\sigma_\gamma=m-\sigma. \tag{B5}$$

Integration over ρ was discussed in detail in Refs. [24,32]:

$$\begin{aligned}I_{ll'}(\varkappa,\varkappa',\varkappa_\gamma)&=\int_0^\infty J_l(\varkappa\rho)J_{l'}(\varkappa'\rho)J_{l-l'}(\varkappa_\gamma\rho)\rho\,d\rho\\&=(-1)^{l'}\frac{\cos(l\beta'+l'\beta)}{2\pi\,\Delta(\varkappa,\varkappa',\varkappa_\gamma)},\end{aligned} \tag{B6}$$

where l and l' are integers, $\Delta(\varkappa,\varkappa',\varkappa_\gamma)$ is the area of the triangle with sides $\varkappa,\varkappa',\varkappa_\gamma$, and β and β' are the angles of this triangle

opposite to $\varkappa$ and $\varkappa'$, respectively. Note that the corresponding expression in Ref. [11], Eq. (3), is incorrect.

The spinorial calculations reduce to the quantity $W^{(\sigma\sigma'\sigma_\gamma)}$ defined in Eq. (A6), which makes it clear that $\sigma_\gamma = \sigma - \sigma'$. Together with Eq. (B5), it leads to the conservation of the z projection of the total angular momentum

$$m' + m_\gamma = m. \tag{B7}$$

The final result for triple-twisted S-matrix element takes a rather compact form

$$S_{3\mathrm{tw}} = -i(2\pi)^{3/2}\sqrt{4\pi\alpha}N_{\mathrm{tw}}N'_{\mathrm{tw}}N^{\gamma}_{\mathrm{tw}}\sqrt{\varkappa\varkappa'\varkappa_\gamma}\,\delta(E'+\omega-E)\delta(p'_z+k_z-p_z)x[2\lambda\sqrt{(E-m_e)(E'+m_e)} + 2\lambda'\sqrt{(E'-m_e)(E+m_e)}]\sum_{\sigma,\sigma'=\pm1/2} d^{1/2}_{\sigma\lambda}(\theta_p)d^{1/2}_{\sigma'\lambda'}(\theta_{p'})d^{\ 1}_{\sigma-\sigma',\lambda_\gamma}(\theta_k)I_{m-\sigma,m'-\sigma'}(\varkappa,\varkappa',\varkappa_\gamma)[2\sigma(\delta_{\sigma\sigma'}-\sqrt{2}\delta_{\sigma,-\sigma'})]. \tag{B8}$$

This S-matrix element is only the first step of the full calculation. One then needs to properly define the final phase space and, after properly regularizing the expression, perform an intricate summation over the final electron values m'. Alternatively, one can take a more physical approach and introduce a superposition of pure Bessel states that would be normalizable in the transverse plane. In any event, the relation of $S_{3\mathrm{tw}}$ to the physically measurable quantities is, to say the least, nontrivial and was discussed at length in Ref. [33].

However, we underline that, for our problem, using the twisted state basis for all three particles is a completely unnecessary complication for two reasons. First, the final electron phase space is always integrated out. Second, whenever we calculate the spectral-angular distribution, we automatically project the final photons on the plane-wave basis. Of course, the final result for the spectral-angular distribution must be the same. However, experience shows that, by choosing an unfortunate calculational approach, one can easily obscure the physics and arrive at wrong conclusions.

[1] P. A. Cherenkov, Dokl. Akad. Nauk SSSR **2**, 451 (1934); S. I. Vavilov, *ibid.* **2**, 457 (1934).
[2] I. M. Frank and I. E. Tamm, Dokl. Akad. Nauk **14**, 107 (1937).
[3] V. L. Ginzburg, Zh. Eksp. Teor. Fiz. **10**, 589 (1940).
[4] A. Sokolov, Dokl. Akad. Nauk SSSR **28**, 415 (1940).
[5] J. M. Jauch and K. M. Watson, Phys. Rev. **74**, 1485 (1948).
[6] V. L. Ginzburg, Sov. Phys. Usp. **2**, 874 (1960).
[7] B. M. Bolotovskii, Sov. Phys. Usp. **4**, 781 (1962).
[8] B. M. Bolotovskii, Sov. Phys. Usp. **52**, 1099 (2009).
[9] V. L. Ginzburg, *Theoretical Physics and Astrophysics* (Pergamon, Oxford, 1979).
[10] G. N. Afanasyev, *Vavilov-Cherenkov and Synchrotron Radiation: Foundations and Applications* (Kluwer Academic, Dordrecht, 2005).
[11] I. Kaminer, M. Mutzafi, A. Levy, G. Harari, H. Herzig Sheinfux, S. Skirlo, J. Nemirovsky, J. D. Joannopoulos, M. Segev, and M. Soljačić, Phys. Rev. X **6**, 011006 (2016).
[12] S. Iablokov, arXiv:1511.05518.
[13] K. Y. Bliokh, Y. P. Bliokh, S. Savel'ev, and F. Nori, Phys. Rev. Lett. **99**, 190404 (2007).
[14] M. Uchida and A. Tonomura, Nature (London) **464**, 737 (2010); J. Verbeeck, H. Tian, and P. Schlattschneider, *ibid.* **467**, 301 (2010).
[15] B. J. McMorran *et al.*, Science **331**, 192 (2011).
[16] G. Guzzinati, Exploring electron beam shaping in transmission electron microscopy, Ph.D. thesis, University of Antwerp, 2015.
[17] I. P. Ivanov and D. V. Karlovets, Phys. Rev. Lett. **110**, 264801 (2013).
[18] I. P. Ivanov and D. V. Karlovets, Phys. Rev. A **88**, 043840 (2013).
[19] V. M. Budnev, I. F. Ginzburg, G. V. Meledin, and V. G. Serbo, Phys. Rep. **15**, 181 (1975).
[20] V. N. Baier, V. S. Fadin, V. A. Khoze, and E. A. Kuraev, Phys. Rep. **78**, 293 (1981).
[21] V. B. Berestetsky, E. M. Lifshitz, and L. P. Pitaevsky, *Quantum Electrodynamics* (Butterworth-Heinemann, Oxford, 1982), Vol. 4.
[22] V. Serbo, I. P. Ivanov, S. Fritzsche, D. Seipt, and A. Surzhykov, Phys. Rev. A **92**, 012705 (2015).
[23] U. D. Jentschura and V. G. Serbo, Eur. Phys. J. C **71**, 1571 (2011).
[24] I. P. Ivanov, Phys. Rev. D **83**, 093001 (2011).
[25] G. Guzzinati, P. Schattschneider, K. Y. Bliokh, F. Nori, and J. Verbeeck, Phys. Rev. Lett. **110**, 093601 (2013).
[26] T. Takahashi, Y. Shibata, K. Ishi, M. Ikezawa, M. Oyamada, and Y. Kondo, Phys. Rev. E **62**, 8606 (2000).
[27] A. P. Potylitsyn, Y. A. Popov, L. G. Sukhikh, G. A. Naumenko, and M. V. Shevelev, J. Phys.: Conf. Ser. **236**, 012025 (2010).
[28] K. Saitoh, Y. Hasegawa, N. Tanaka, and M. Uchida, J. Electron Microsc. (Tokyo) **61**, 171 (2012).
[29] M. E. Rose, *Elementary Theory of Angular Momentum* (Wiley, New York, 1957).
[30] D. A. Varshalovich, A. N. Moskalev, and V. K. Khersonskii, *Quantum Theory of Angular Momentum* (World Scientific, Singapore, 1988).
[31] O. Matula, A. G. Hayrapetyan, V. G. Serbo, A. Surzhykov, and S. Fritzsche, J. Phys. B **46**, 205002 (2013).
[32] A. Gervois and H. Navelet, J. Math. Phys. (N.Y.) **25**, 3350 (1984).
[33] I. P. Ivanov and V. G. Serbo, Phys. Rev. A **84**, 033804 (2011).